Optimization

A Journal of Mathematical Programming and Operations Research

ISSN: 0233-1934 (Print) 1029-4945 (Online) Journal homepage: http://www.tandfonline.com/loi/gopt20

Combined time and energy optimal trajectory planning with quadratic drag for mixed discrete-continuous task planning

Ayal Taitler, Ilya Ioslovich, Per-Olof Gutman & Erez Karpas

OPTIMIZATION
https://doi.org/10.1080/02331934.2018.1502769

Taylor & Francis
Taylor & Francis Group

Check for updates

Combined time and energy optimal trajectory planning with quadratic drag for mixed discrete-continuous task planning

Ayal Taitler [a], Ilya Ioslovich [b], Per-Olof Gutman [b] and Erez Karpas [c]

[a] Technion Autonomous Systems Program, Technion Israel Institute of Technology, Haifa, Israel; [b] Faculty of Civil and Environmental Engineering, Technion Israel Institute of Technology, Haifa, Israel; [c] Faculty of Industrial Engineering and Management, Technion Israel Institute of Technology, Haifa, Israel

ABSTRACT

The problem of mixed discrete-continuous task planning for mechanical systems, such as aerial drones or other autonomous units, can be often treated as a sequence of point-to-point trajectories. In this work, the problem of optimal trajectory planning under a combined completion time and energy criterion, for a straight point to point path for a second-order system with quadratic under state (velocity) and control (acceleration) constraints is considered. The solution is obtained and proved to be optimal using the Pontryagin Maximum Principle. Simulation results for different cases are presented and compared with a customary numerical optimal control solver.

ARTICLE HISTORY
Received 7 May 2018
Accepted 12 July 2018

KEYWORDS
Optimal control; Pontryagin Maximum Principle; minimum time; minimum energy

1. Introduction

Robots operating in the real world often have to come up with a sequence of actions which will take them from an initial state to a desired goal state. During planning the robots have to take into account both discrete and continuous changes, e.g. temporal constraints. Temporal planners such as [1] and [2] have been introduced in the last few years and managed to deal with the temporal problems quite well. When dealing with robots, dynamic properties such as accelerations and continuity of motion (e.g. continuous velocity) are an integral part of the problem. The temporal planning framework can represent these requirements to some degree, assuming a low-level controller can compensate for any inaccuracies done during the planning process. An attempt to address the problem of finding a discrete temporal plan with a continuous control policy within the planning framework has been done in Scotty [3]. In that planner, a constant velocity profile was found which obeys simple physical constraints such as

CONTACT Ilya Ioslovich agrilya@technion.ac.il

bounded velocity, but no physical continuity between actions has been enforced. Thus the policy planned is only a rough reference trajectory for a physical system to follow, but it is a step towards simultaneous discrete-continuous planning. One of Scotty's advantages is the fact that the planning is done for a first-order integrator, which is very simple and allows Scotty to formulate a simple second-order cone optimization problem which can be solved efficiently. The next logical step is to make planners like Scotty aware of more complex dynamic constraints in order to find a more realistic trajectory while still keeping the simplicity of the planning with a first-order integrator.

The planner discussed so far usually calculates a sequence of piecewise linear trajectories, where each line corresponds to a temporal action in the plan. Thus each trajectory is in fact a single axis trajectory from an initial condition to a final condition, which are imposed by the actions before and after. Planning with a simple high-level model such as done in Scotty with a low-level planner which uses more realistic and complex dynamics can keep the simplicity of the planning and still make it more aware of the real dynamics. Of course the low-level planner will have to be able to verify and impose constraints as necessary on the high-level simple planner.

In this work, we address the problem of planning a single trajectory for a model with constraints, which were inspired by the requirements of Scotty, so that a mixed discrete-continuous planner can be used during the planning process. A method for computing the optimal trajectory for a combined minimum completion time and minimum energy is given, based on a second-order integrator with quadratic drag, subject to constraints. The control input is the acceleration which enforces a continuous velocity profile and is bounded as expected. The velocity is also bounded and the quadratic drag which is proportional to the velocity square is both inspired by the battery requirements of Scotty and of real drag operating on objects moving through air or fluids [4].

The general problem of optimal control has been studied extensively and solid mathematical tools have been established [5], and later extended even more, e.g. problems with state constraints [6]. The problems of optimal time and optimal energy are particularly of interest, especially for trajectory planning problems, and many approaches have been established [7]. In [8], a solution for second-order and third-order models with control and state constraints for a time optimal criterion, with a drag which was proportional to the sign of the velocity has been presented. In [9], the problem of minimum energy for a third-order system with control and state constraints was considered, and [10] has considered a similar problem with additional energy terms such as the mechanical energy loss. A comparison between a minimum energy criterion and a minimum time criterion was done in [11]. Combined criteria for robotic manipulators were considered in [12] for linear dynamics with path constraints. An Second-Order Cone Programing (SOCP) optimization approach for combined criteria was introduced in [13] for dynamics with a quadratic term without path constraints. A numerical tool for solving optimal control problem is DIDO [14], which by using pseudo-spectral algorithms [15] can target complex optimal control problems. This solver will be used for comparison of the results in this work.

The solution presented here for the combined time-energy criterion for a second-order system with quadratic drag and path constraints has two possible solutions based on the parameters of the problem. One of the solutions has a time optimal like characteristics, comprising of three segments: acceleration, constant velocity on the bound and deceleration. The other solution is more like a minimum energy solution comprised of a single arc not reaching the bounds. The optimization problem is presented in Section 3 and solved in Section 4, simulation results and comparison to a well-established commercial solver are presented in Section 6, and conclusions are presented in Section 7.

2. Background material

We consider a standard optimal control formulation in continuous time. The goal is to minimize a performance criterion under some system dynamics, and control and state constraints with known starting and final conditions. The optimization problem is of the following general form:

$$\begin{aligned} &\underset{u,t_f}{\text{minimize}} \quad \int_{t_0}^{t_f} l(x,u)\,\mathrm{d}t \\ &\text{subject to} \\ &\qquad \frac{\mathrm{d}x}{\mathrm{d}t} = f(x,u) \\ &\qquad x(t_0) = x_0 \\ &\qquad x(t_f) = x_f \\ &\qquad C_u u \le U \quad t \ge t_0 \\ &\qquad Cx \le X \quad t \ge t_0. \end{aligned} \tag{1}$$

Here $x \in \mathbb{R}^n$ is the state vector, and $u \in \mathbb{R}^2$ is the control input to the system, both are functions of the time. The function $f(x,u)$ is the system dynamics and U and X are the constraints on the control and state vector respectively. The Hamiltonian of the system is defined as

$$H_o(x,p,u) = p^{\mathrm{T}} f(x,u) - l(x,u), \tag{2}$$

where $p \in \mathbb{R}^n$ is the vector of co-states. When state vector constraints are present the augmented Hamiltonian is used

$$H(x,p,u,\lambda) = p^{\mathrm{T}} f(x,u) - l(x,u) - \lambda^{\mathrm{T}}(Cx - X), \tag{3}$$

where $\lambda \ge 0$ is a vector of time-dependent Lagrange multipliers which are non-zero only when the respective state constraint is active. The optimal solution

x^*, u^*, p^* must satisfy three conditions. The first is the system dynamics

$$\frac{\mathrm{d}x^*}{\mathrm{d}t} = \frac{\partial H(x^*, p^*, u^*, \lambda^*)}{\partial p}. \tag{4}$$

The second is the co-states dynamics

$$\frac{\mathrm{d}p^*}{\mathrm{d}t} = -\frac{\partial H(x^*, p^*, u^*, \lambda^*)}{\partial x}, \tag{5}$$

and the third condition is for the control vector

$$H(x^*, p^*, u^*, \lambda^*) = \max_u H(x^*, p^*, u, \lambda^*). \tag{6}$$

According to the transversality condition for the free final time [16]

$$H(t_f) = 0. \tag{7}$$

Finally, when the Hamiltonian is not explicitly time dependent, $\partial H/\partial t = 0$ [16], we conclude that

$$H(t_f) = 0. \tag{8}$$

The Hamiltonian is constant through the whole process.

3. Statement of the problem

The system considered is a second-order integrator with quadratic drag, under acceleration/control constraint and velocity/state constraint. The chosen performance measure is one combined of completion time and consumed energy. It is obvious that the two are conflicting and cannot be met simultaneously. The trade-off between the two components in the criterion are tuned with a weight parameter α in order to give more significance to one of them.

The state equations, performance measure, boundary conditions and constraints are given next

$$\underset{u,t_f}{\text{minimize}} \quad \int_{t_0}^{t_f} \left(1 + \alpha\frac{1}{2}u^2(t)\right) \mathrm{d}t, \quad \alpha > 0$$

subject to

$$\begin{aligned} &\frac{\mathrm{d}x_1}{\mathrm{d}t} = x_2 \\ &\frac{\mathrm{d}x_2}{\mathrm{d}t} = u - \frac{1}{2}kx_2^2 \\ &|u| \le U \quad t \ge t_0 \\ &|x_2| \le V \quad t \ge t_0 \\ &x_1(t_0) = x_{10},\ x_2(t_0) = x_{20} \\ &x_1(t_f) = x_{1f},\ x_2(t_f) = x_{2f}. \end{aligned} \tag{9}$$

Here x_1 is the distance, measured in metres [m], x_2 is the velocity, measured in metres per second [m/s], u is the acceleration, measured in metres per square seconds [m/s^2], k is the drag coefficient, U and V are the bounds on the acceleration and the velocity respectively. The weight α is a designer degree of freedom as required, it tunes the importance of the control effort or energy consumption compared with the completion time. For $\alpha \to 0$, we expect to approach a minimum time solution.

4. Optimization

The solution for this problem is divided into two cases, distinguished by the status of the constraint on the velocity along the trajectory. The constraint on the control also induces more cases, i.e. if the control constraint is active or not, but they are dealt with within the scope of the two velocity cases.

We assume that the velocity is not reversed during the process, thus $x_2 \geq 0$ automatically, thus according to the state equation for x_2 the maximum sustainable velocity under the control input constraint U is when $\mathrm{d}x_2/\mathrm{d}t = 0$. That velocity corresponds to $\sqrt{2U/k}$, thus we shall require

$$V \leq \sqrt{\frac{2U}{k}}. \tag{10}$$

4.1. Solution with active upper bound velocity constraint

In this section, we assume that the constraint on the velocity will be active at some interval along the trajectory.

We also assume that the lower bound on x_2 can be omitted, and only the upper bound may be active, i.e. any trajectory with zero or negative velocity is not feasible. The appropriate Hamiltonian of the problem is then

$$H = p_1 x_2 + p_2 \left(u - \frac{1}{2} k x_2^2 \right) - 1 - \alpha \frac{1}{2} u^2 - \lambda_2 (x_2 - V). \tag{11}$$

According to the transversality condition and the condition for free final time, we obtain that

$$H \equiv 0. \tag{12}$$

The time-dependent value λ_2 is a Lagrange multiplier for the constraint on the upper bound of the velocity x_2. Note that $\lambda_2 \geq 0$, and may be nonzero only when the velocity constraint is active, i.e. $x_2 = V$. At all other times, λ_2 must be zero. The co-states equations are $\mathrm{d}p/\mathrm{d}t = \partial H/\partial x$, specifically

$$\begin{aligned} \frac{\mathrm{d}p_1}{\mathrm{d}t} &= 0, \\ \frac{\mathrm{d}p_2}{\mathrm{d}t} &= -p_1 + p_2 k x_2 + \lambda_2. \end{aligned} \tag{13}$$

The maximization of H over u yields

$$\frac{\partial H}{\partial u} = p_2 - \alpha u = 0 \quad \Rightarrow \quad u = \frac{p_2}{\alpha},\ |u| \le U. \tag{14}$$

And in order to satisfy the control u is

$$u = \min\left(\frac{p_2}{\alpha}, U \cdot \operatorname{sgn}(p_2)\right). \tag{15}$$

We assume that at the beginning of the movement, i.e. on some interval $[t_0, t_1]$, the velocity x_2 is not on the boundary, i.e. $x_2 < V$. From Equation (13), we see that p_1 is constant, and we assume it is positive. We assume that at time $t \in [t_0, t_1]$, we have $\mathrm{d}p_2/\mathrm{d}t < 0$, $p_2 \ge 0$ and $\mathrm{d}x_2/\mathrm{d}t > 0$ because p_2 is proportional to the control. During this interval, the system accelerates, so the control is positive and the velocity is increasing. When x_2 reaches the upper bound V at some time t_1, we should have $\mathrm{d}p_2(t)/\mathrm{d}t|_{t=t_1} = 0$, because of the constraint on the velocity, the control must be constant and thus p_2 must be constant. Therefore it follows from Equation (13) that at time t_1 we have

$$-p_1 + p_2(t_1)kV + \lambda_2 = 0. \tag{16}$$

Since at this time the velocity has reached its upper bound, we should have

$$\left.\frac{\mathrm{d}x_2(t)}{\mathrm{d}t}\right|_{t=t_1} = 0. \tag{17}$$

Moreover, on the interval $t \in [t_1, t_2]$, the velocity is constant which implies that the control is constant, which means Equation (14) holds. Thus at time t_1

$$\frac{\mathrm{d}x_2(t)}{\mathrm{d}t}|_{t=t_1} = u(t_1) - \frac{k}{2}x_2(t_1)^2 = \frac{p_2(t_1)}{\alpha} - \frac{k}{2}V^2 = 0, \tag{18}$$

which yields

$$p_2(t_1) = \alpha\frac{k}{2}V^2. \tag{19}$$

From this time point, the co-state p_2 must be constant on the interval $[t_1, t_2]$ for $x_2 = V$, and the Lagrange multiplier λ_2 should be non-negative in order to keep $\mathrm{d}p_2(t)/\mathrm{d}t = 0$ for $t \in [t_1, t_2]$. So, from Equations (16) and (19) we obtain

$$\lambda_2 = p_1 - \alpha\frac{k^2}{2}V^3. \tag{20}$$

The value of the constant co-state p_1 can be found from the conditions $H(t_1) = 0$, $x_2(t_1) = V$, and Equations (14) and (19). We have

$$H(t_1) = p_1 V - 1 - \alpha\frac{k^2}{8}V^4, \tag{21}$$

which yields

$$p_1 = \frac{1}{V} + \alpha \frac{k^2}{8} V^3. \tag{22}$$

Substituting Equation (22) into Equation (20) yields

$$\lambda_2 = \frac{1}{V} - \alpha \frac{3k^2}{8} V^3 \geq 0. \tag{23}$$

The inequality in (23) denotes the condition for the upper bound of the velocity V to be reachable. If this inequality is not valid then the assumption that the velocity reaches the upper bound does not hold, and the trajectory has a different structure. In this case, another procedure is needed to be discussed in Section 4.2. So far we have obtained the values of the constant p_1 and of x_2 and p_2 at times t_1 and t_2 since $[t_1, t_2]$ is a constant velocity interval.

The maximal value of the upper constraint for the velocity is found from Equation (23) as the positive root of

$$\bar{V} = \left(\frac{8}{3\alpha k^2} \right)^{1/4}. \tag{24}$$

Thus a necessary condition for the velocity to reach its maximal value is

$$V < \bar{V}. \tag{25}$$

Note, however, that this condition is necessary but not sufficient for the existence of the solution with an interval at the upper velocity bound. In the reminder of this section, it is assumed that (25) is satisfied. In order to obtain the trajectory on the interval $[t_0, t_1]$, we can integrate backward the states and co-states equations from $x_2(t_1) = V$ to $x_2(t_0) = x_{20}$. Thus we can determine the value $x_1(t_1) - x_1(t_0)$ and $u(t)$ on the interval $[t_0, t_1]$, and the value of t_1. The value $t = t_2$ when the trajectory should leave the upper value for x_2 must be found by first calculating the trajectory on the time interval $[t_2, t_f]$. The trajectory on the last interval $[t_2, t_f]$ can be found similarly by integrating forward from $x_2(t_2) = V$ to $x_2(t_f) = x_{2f}$. This way we can determine the control u on the interval $[t_2, t_f]$, and the length of the last interval $t_f - t_2$. We can also determine $x_1(t_f) - x_1(t_2)$. The last thing to do is to determine the middle segment of the trajectory which is according to

$$t_2 - t_1 = \frac{x_1(t_2) - x_1(t_1)}{V}. \tag{26}$$

Note that at some point or duration along the trajectory the control $u(t)$, as described in Equation (14), may exceed its bound according to (9). In this case, the control input saturates on its bound (15), i.e. if $|p_2| > \alpha U$, then Equation (13) proceeds as is, but the state equation for x_2 has a constant value for u, in compact form the equation for x_2 becomes

$$\frac{\mathrm{d}x_2}{\mathrm{d}t} = \min\left(U, \frac{p_2}{\alpha}\right) - \frac{1}{2}kx_2^2 \tag{27}$$

for positive p_2, and

$$\frac{\mathrm{d}x_2}{\mathrm{d}t} = \max\left(-U, \frac{p_2}{\alpha}\right) - \frac{1}{2}kx_2^2 \tag{28}$$

for negative p_2.

4.2. Solution with non-active upper bound velocity constraint

When the value V cannot be achieved, there cannot be solution with a steady-state interval where the velocity is constant and $x_2 \in [0, V)$. Such a solution would imply that $\mathrm{d}p_2(t)/\mathrm{d}t = 0$ on an interval where $\lambda_2 = 0$ since the upper velocity bound is not active, and since p_2 has continuous smooth dynamics (13) this will contradict the uniqueness and existence theorem for ODE [17]. Let us denote the unknown value of $\max x_2$ as V_m, and $t_1 = \operatorname{argmax}_t x_2$. In this case, we have $t_1 = t_2$ since as just shown, there is no interval when $x_2(t) = V_m < V$. At $t = t_1$, the variable p_2 should continue to decrease, $\mathrm{d}x_2(t)/\mathrm{d}t|_{t=t_1} = 0$, and $p_2 > 0$. Equations (19) and (22) are still valid, but with $V = V_m$. Integrating state and co-state equations backward and forward until $x_2 = x_{20}$ and $x_2 = x_{2f}$, respectively, we get p_1 and thus control u both for $[t_0,\ t_1]$ and $[t_1,\ t_f]$. However, now the variable x_1 has residual

$$res = (x_1(t_f, V_m) - x_{1f})^2, \tag{29}$$

which is a function of V_m. In order to do the calculation we need an initial guess for V_m.

We choose $\bar{V}$ from Equation (24) as the initial guess. Now we should minimize this residual in Equation (29) and thus find a true value of V_m. It is clear that the minimum of this residual is zero.

4.3. Solution with active upper bound velocity constraint for short paths

In the case where $V < \bar{V}$, but the final condition $x_1(t_f)$ is small, such that the system does not have enough time to accelerate to the maximum velocity and decelerate in order to satisfy the final condition we also do not have a constant velocity interval. In this case, we have a similar trajectory structure as described in Section 4.2. The same assumptions hold in this case also, but with a different initial guess for V_m. The condition on V is automatically satisfied here, and it does not depend on the initial and final conditions. We know that the maximum velocity must satisfy Equation (10), so we can choose as an initial guess V_m from this equation. Again it is clear that the minimum of the residual is zero.

Now we have everything we need to find t_f and the control signal u for the complete motion.

5. Marginal cases

There are two cases of interest when analysing the performance measure in (9). The first is when we take $\alpha \to 0$ and the second is when α is very large; we should be cautious when defining the problem for $\alpha \to \infty$.

5.1. Minimum time

When taking $\alpha \to 0$, we get from the performance measure

$$\min J = \int_{t_0}^{t_f} \left(1 + \alpha \frac{1}{2} u^2(t)\right) \mathrm{d}t = t_f + \alpha \frac{1}{2} \int_{t_0}^{t_f} u^2(t)\,\mathrm{d}t. \tag{30}$$

And since u is bounded on the finite interval $[t_0, t_f]$, we expect the solution of the problem to look like the solution of the time minimum problem

$$\min J = t_f = \int_{t_0}^{t_f} 1 \cdot \mathrm{d}t. \tag{31}$$

Taking $\alpha \to 0$ in Equation (15), thus assuming $p_2 \gg \alpha$ results in

$$u = \min\left(\frac{p_2}{\alpha}, U \cdot sgn(p_2)\right) = U \cdot sgn(p_2). \tag{32}$$

The last does not hold when p_2 is small, this happens in the region where p_2 approaches zero, or right when p_2's value decreases from zero. As $\alpha \to 0$ so does the length of the region where p_2 is close to zero, goes as well to zero. It is clear that the system will accelerate with saturated u to the maximum velocity V, stay on the maximum velocity as long as needed, and then decelerate at minimum u to the final condition. The transitions from maximum acceleration to zero acceleration, and again from zero acceleration, would have been instantaneous if $\alpha = 0$, i.e. pure minimum time, but for $\alpha \to 0$ will have some length greater than zero. Thus the trajectory has the form of almost a Bang–Constant–Bang with small transitions. In the system described in (3), the drag prevents the control from staying at zero, or the velocity will be reduced. So, in this case the constant value of u is the value of the control that makes $\mathrm{d}x_2/\mathrm{d}t = 0$, specifically

$$\tilde{u} = \frac{1}{2} k V^2. \tag{33}$$

Note that when V is high or the time for the motion is short, the system will not manage to reach the velocity bound before it will have to switch the control to the negative value. In this case, the profile will be simply close to a Bang–Bang profile of maximum acceleration, maximum deceleration and a small transition between the two which as explained previously goes to zero as $\alpha \to 0$.

5.2. Minimum energy

When taking $\alpha \to \infty$, it is important to fix t_f, otherwise the solution will be one of $u \to 0$ and $t_f \to \infty$. Thus when t_f is fixed the performance measure is

$$\min J = t_f + \alpha \frac{1}{2} \int_{t_0}^{t_f} u^2(t)\, \mathrm{d}t = t_f + \alpha \hat{J}, \tag{34}$$

where

$$\hat{J} = \frac{1}{2} \int_{t_0}^{t_f} u^2(t)\, \mathrm{d}t. \tag{35}$$

It is clear that the following holds:

$$\operatorname{argmin}_u J = \operatorname{argmin}_u \hat{J}. \tag{36}$$

Equation (35) is the standard minimum energy criterion. In order to solve that, we observe that Equation (10) still holds, where the Hamiltonian now is

$$H = p_1 x_2 + p_2 \left(u - \frac{1}{2} k x_2^2 \right) - \frac{1}{2} u^2 - \lambda_2 (x_2 - V). \tag{37}$$

From maximization of the Hamiltonian over u, it follows that $u = p_2$ when not on the state constraint, and $u = (k/2) V^2$ when on the state constraint. Equation (17) still holds, and it follow from it that $p_2(t_1) = (k/2) V^2$. Now the solution is easily obtained similarly to the method described in Section 4.1. However, here we do not have the property $H = 0$ because of the fixed time, but $H = c$ where c is an unknown constant. The Hamiltonian at time $t = t_1$ is

$$H(t_1) = p_1 V - \frac{k^2}{8} V^4 = c, \tag{38}$$

which yields

$$p_1 = \frac{c}{V} + \frac{k^2}{8} V^3. \tag{39}$$

When not on the state constraint, we denote again the maximal velocity as V_m. The constant c and the maximum velocity V_m are unknowns and should be found from the minimization of residuals. Initial guesses for c and V_m are needed and can be taken to be the same as in Section 4.1. We should integrate states and co-states equations backward until $x_2 = x_{20}$ and forward until $t = t_f$. Note that the final time t_f is fixed here, and thus the integration is until that time and not the final condition x_{2f}. Thus we obtain the fixed time residual

$$res = \alpha_1 \cdot (x_1(c, V_m) - x_{1f})^2 + \alpha_2 \cdot (x_2(c, V_m) - x_{2f})^2. \tag{40}$$

Here α_1, α_2 are suitable weighting coefficients. Minimizing that residual yields c and V_m, and consequently p_1, and the control for the time interval $[t_0, t_f]$.

When on the state constraint the residual is a function of c only since $V = V_m$. We should integrate states and co-states equations backward until $x_2 = x_{20}$ and forward until $x_2 = x_{2f}$. The time interval of the middle segment can be determined according to

$$t_2 - t_1 = t_f - t_1 - t_3. \tag{41}$$

Here, t_1 denotes the time length of the first segment and t_3 denotes the time length of the third segment. The appropriate residual in this case is

$$res = \alpha_1 \cdot (x_1(c) - x_{1f})^2 + \alpha_2 \cdot (x_2(c) - x_{2f})^2. \tag{42}$$

Again α_1, α_2 are suitable weighting coefficients. Minimizing this residual yields c, and the control for the time interval $[t_0, t_f]$.

6. Simulations

We demonstrate the solution obtained for the different cases. The solutions are compared to DIDO, a widely used commercial numerical solver for optimal control problems. The number of nodes used in the DIDO simulations was 30. All simulation were done with Matlab 2015b on an i5-core Intel computer with 4GB of RAM. The values for the simulation were taken to be values compatible with a physical problem drones. In all simulations, three graphs are presented, the distance, velocity and acceleration profiles as computed by the two algorithms, one on top of the other to show the agreement and difference between the two. DIDO solution is shown in thin red line with asterisks, and the explicit solution is in thick blue.

The first simulation is for the case where the condition on the velocity bound equation (25) is satisfied. The drag coefficient is standard for a flying aircraft and set to be $k = 0.05$. The tuning parameter α is set to be in scale between the energy and the time, $\alpha = 0.01$. Thus when substituting in Equation (24) we obtain in this case that $\bar{V} = 18.072[\mathrm{m/s}]$. The bound on the velocity then is chosen to be $V = 9[\mathrm{m/s}]$ and the bound on the acceleration is $U = 10[\mathrm{m/s^2}]$. The initial and final conditions for the motion are respectively $x_0 = [0, 1]^{\mathrm{T}}$ and $x_f = [20, 4]^{\mathrm{T}}$. The result is presented in Figure 1. In this case, there is almost a perfect match between the two algorithms. The system accelerates until the bound on the velocity, then the system maintains a constant velocity on an intermediate interval where the control is not zero due to the drag, and finally the system decelerates to the final condition. A saturation in the control is also present at the first part of the motion due to the active constraint on the acceleration in that part. The constant velocity interval length is $t_2 - t_1 = 0.5347[\mathrm{s}]$, where $t_1 = 1.2857[\mathrm{s}]$ and $t_2 = 1.8205[\mathrm{s}]$. The final time for the motion calculated by the explicit solution is 2.7965[s], and the cost is 3.3333, DIDO's final time is 2.7971[s], and the cost is 3.3291. The differences are negligible and can be attributed to numerical errors.

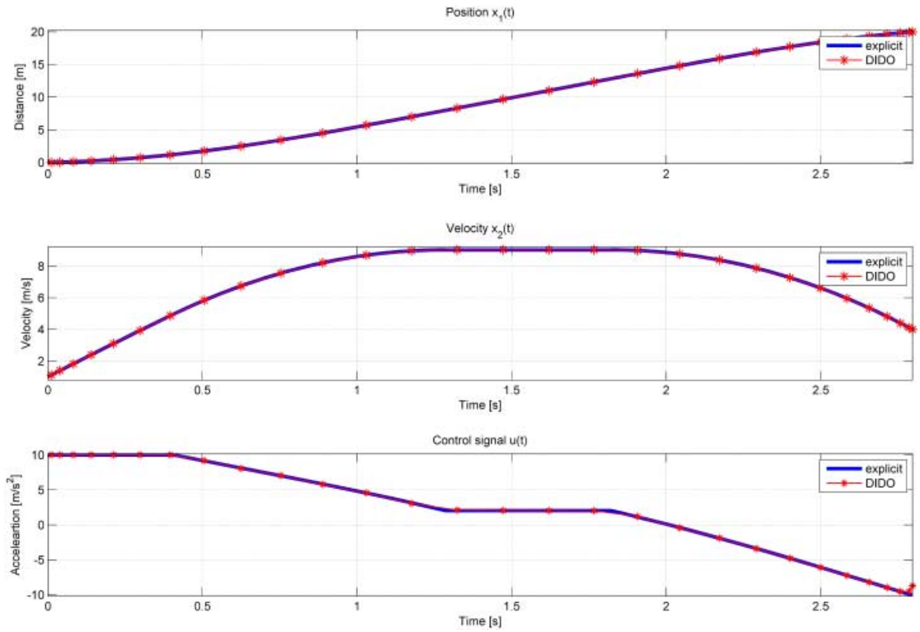

Figure 1. Trajectory with active velocity bound constraint and active acceleration bound constraint.

The second simulation is for the case where the condition on the velocity bound equation (25) is not satisfied. All values but the velocity bound are the same for this simulation, $U = 10[\mathrm{m/s}^2], k = 0.05, \alpha = 0.01, x_0 = [0, 1]^{\mathrm{T}}, x_f = [20, 4]^{\mathrm{T}}$. The velocity is changed so $V > \bar{V}$, hence we choose $V = 36[\mathrm{m/s}]$. The result is presented in Figure 2. Again there is almost a perfect match between the two algorithms. Since the condition for the velocity bound is not satisfied, the system accelerated to a maximum value which is lower then $\bar{V}$ and immediately decelerates to the final condition. The maximum velocity obtained in this example was $x_{2\_max} = 10.2337[\mathrm{m/s}]$ at $t_1 = t_2 = 1.4893[\mathrm{s}]$. Again a saturation in the control is present in the first part of the motion and at the end of the motion. The final time for the motion calculated by the explicit solution is 2.6621[s], and the cost is 3.3074, DIDO's final time is 2.6639[s], and the cost is 3.2981. Again the differences are negligible and can be attributed to numerical errors.

The third simulation is for the case where the condition on the velocity bound equation (25) not satisfied but the path is too short in order for the system to reach the velocity bound. The value for the bound on the velocity is changed back such that $V = 9[\mathrm{m/s}]$, and the final condition is for a short path, i.e. $x_f = [2, 3]^{\mathrm{T}}$. The rest of the values are as in the previous simulation, $U = 10[\mathrm{m/s}^2], k = 0.05, \alpha = 0.01, x_0 = [0, 1]^{\mathrm{T}}$. The result is presented in Figure 3. As in the previous cases, there is almost a perfect match between the two algorithms. The condition on the velocity bound is satisfied so the system is expected to accelerate to the bound and to obtain a trajectory similar to the trajectory presented in Figure 1. Since the

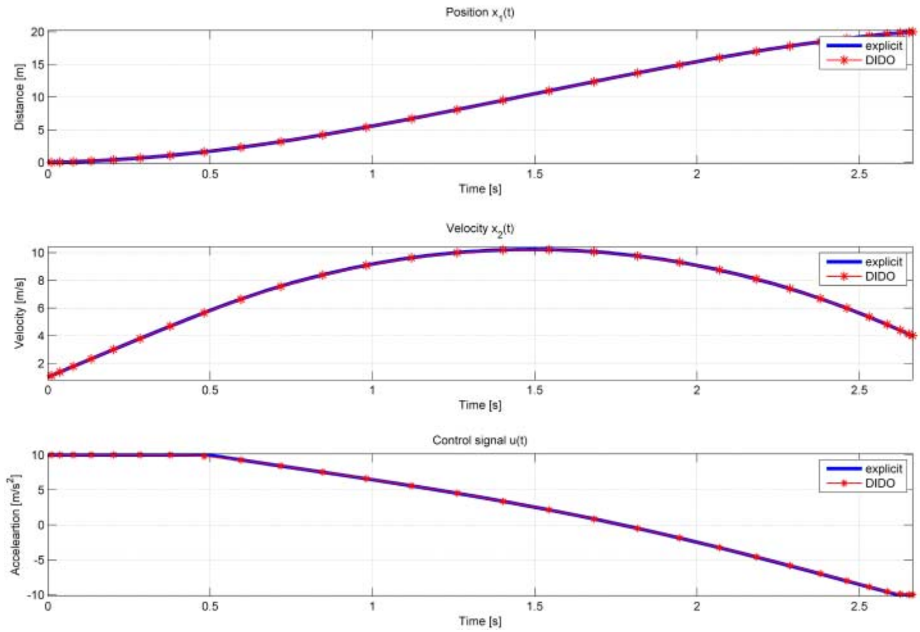

Figure 2. Trajectory with inactive velocity bound constraint and active acceleration bound constraint.

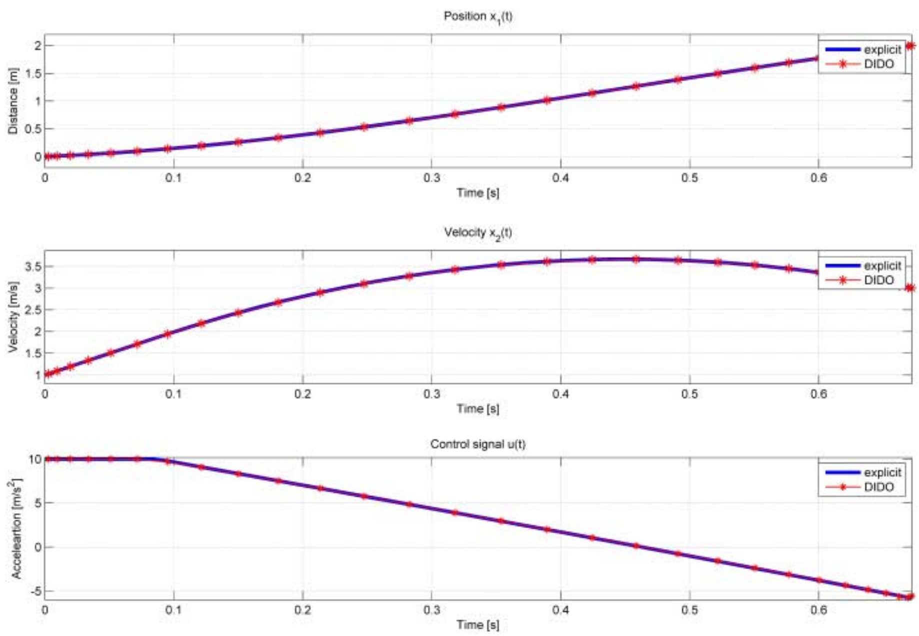

Figure 3. Short path trajectory, velocity condition for reaching the velocity bound is satisfied, but the bound is not reached. The acceleration bound constraint is active.

path for the motion is short the system's velocity does not reach the maximum value and the profile is similar to the profile shown in Figure 2, consisting of two segments, acceleration and deceleration. The maximum velocity obtained in this example was $x_{2\_\max} = 3.6653[\mathrm{m/s}]$ at $t_1 = t_2 = 0.4505[\mathrm{s}]$. A saturation in the control is present in the first part of the motion. The final time for the motion calculated by the explicit solution is 0.6716[s], and the cost is 0.7967, DIDO's final time is 0.6719[s], and the cost is 0.7897. The differences are negligible here also.

The following four simulations are for the marginal cases. The first of the marginal cases to be presented is the case where $\alpha \to 0$, which is expected to look like a minimum time profile. The value chosen for the tuning parameter is $\alpha = 0.00001$. The drag coefficient is $k = 0.05$, the velocity bound is chosen to be low $V = 10[\mathrm{m/s}]$, the acceleration bound is $U = 10[\mathrm{m/s^2}]$, and the initial and final conditions are respectively $x_0 = [0, 1]^{\mathrm{T}}, x_f = [20, 4]^{\mathrm{T}}$. The result is presented in Figure 4. In contrast to previous cases, now we can observe a slight difference between the explicit solution and DIDO's solution, seen mainly in the third plot for the control signal when the control is changed sharply. The trajectory is almost a Bang–Constant–Bang as explained in Section 5.1. The system accelerates at maximum acceleration, upon reaching the velocity bound the system maintains the bound with a constant control signal only to resist the drag, and then decelerates to the final condition at maximum deceleration. The transition regions are almost indistinguishable due to the small value of α. The constant velocity interval length was $t_2 - t_1 = 1.0604[\mathrm{s}]$, where $t_1 = 0.9994[\mathrm{s}]$

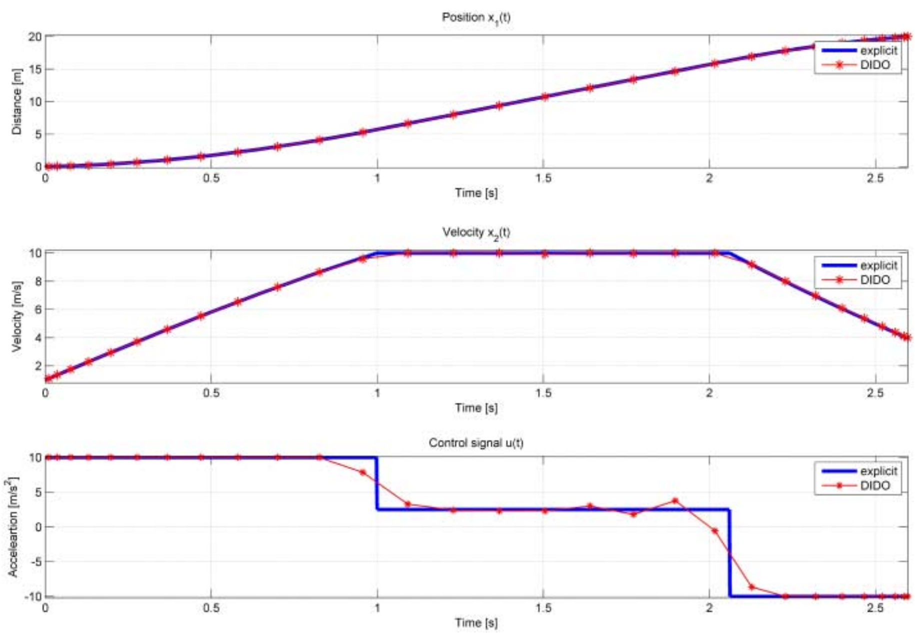

Figure 4. Marginal case with $\alpha \to 0$, minimum time Bang–Constant–Bang profile with active velocity and acceleration bound constraints.

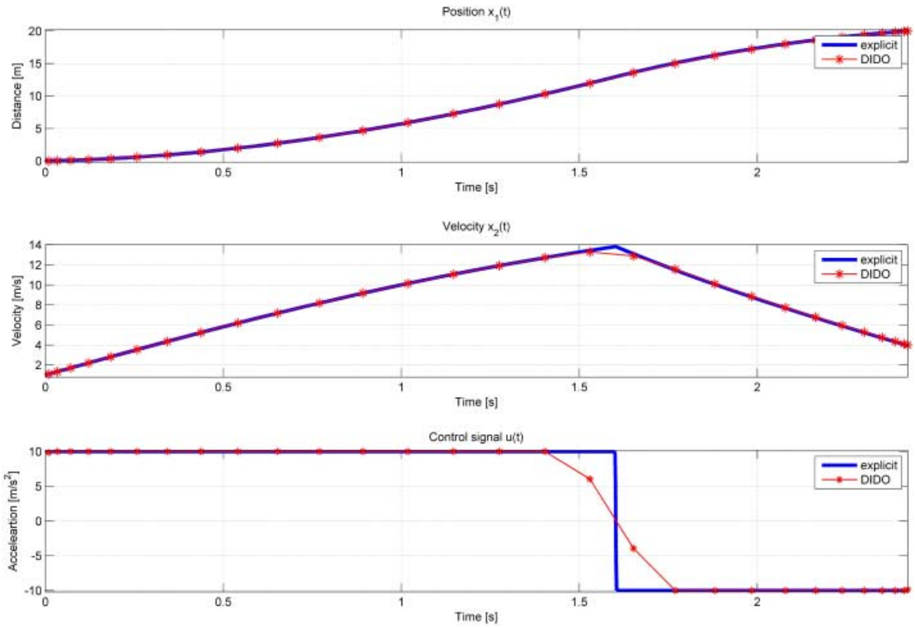

Figure 5. Marginal case with $\alpha \rightarrow 0$, minimum time Bang–Bang profile with active velocity and acceleration bound constraints.

and $t_2 = 2.0598$[s]. The final time for the motion calculated by the explicit solution is 2.5929[s], and the cost is 2.5937, DIDO's final time is 2.5965[s], and the cost is 2.5972. The differences are negligible here also.

The second simulation for the marginal cases is again when $\alpha \rightarrow 0$, but with a much higher velocity bound. All parameters and condition except the bound on the velocity are in the previous simulation, i.e. $U = 10[\mathrm{m/s^2}], k = 0.05, \alpha = 0.00001, x_0 = [0, 1]^{\mathrm{T}}, x_f = [20, 4]^{\mathrm{T}}$, and the velocity bound is set to be $V = 40[\mathrm{m/s}]$. The result is presented in Figure 5. As in the previous case there is a slight difference between the algorithms when the control changes sharply, in both cases the general profile is the same and only in areas where the changes are sharp the differences are observed, due to that we can conclude that they are occurring in result of numerical inaccuracies in DIDO's numerical solver. The trajectory in this case is almost a Bang–Bang, since the maximum velocity is not reached before the system has to decelerate to the final condition. The transition region between the bangs here is visible by the small breaks in the blue line, which otherwise would have been completely straight The maximum velocity obtained here is $x_{2\_\max} = 13.8272[\mathrm{m/s}]$ at $t_1 = t_2 = 1.6016$[s]. The final time for the motion calculated by the explicit solution is 2.4176[s], and the cost is 2.4188, DIDO's final time is 2.4221[s], and the cost is 2.4232. The differences are negligible here also.

The third simulation for the marginal cases is for a fixed time trajectory, when in effect the problem become a minimum energy problem with no α. The bound

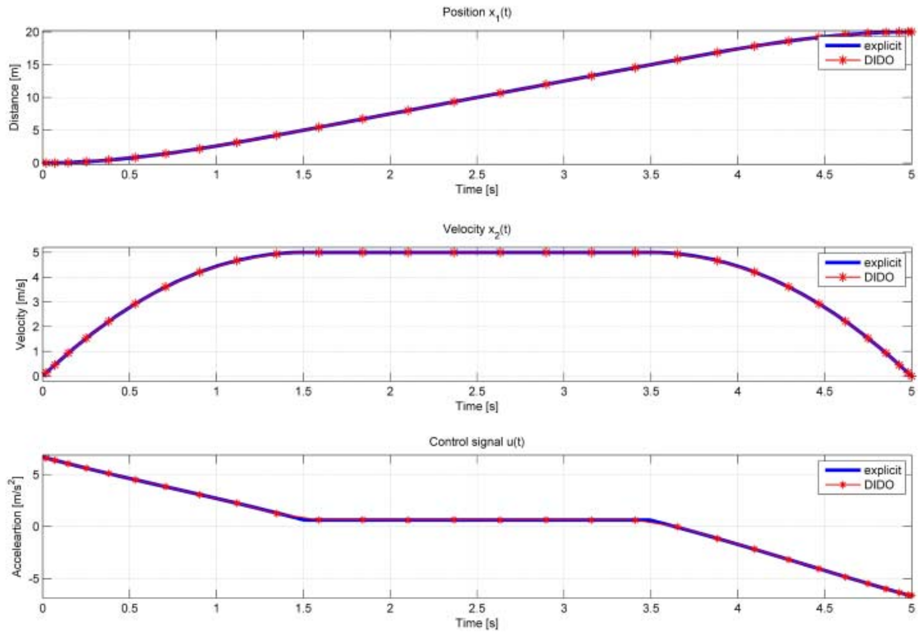

Figure 6. Marginal case with fixed final time, $t_f = 5$, minimum energy profile with active velocity bound constraint.

on the velocity here is chosen to be low so the constraint will become active, i.e. $V = 5[\mathrm{m/s}]$, the control constraint is $U = 10[\mathrm{m/s^2}]$, the initial and final conditions are respectively $x_0 = [0,0]^{\mathrm{T}}, x_f = [20,0]^{\mathrm{T}}$, and the final time is set to be $t_f = 5[s]$. Notice that there is no need for α in this problem. The result is presented in Figure 6. A perfect match between the two algorithms can be observed in this case. The system accelerates to the velocity bound, maintains a constant velocity interval and decelerates to the final condition. The constant velocity interval length was $t_2 - t_1 = 1.9883[\mathrm{s}]$, where $t_1 = 1.5059[\mathrm{s}]$ and $t_2 = 3.4943[\mathrm{s}]$. It is also interesting to note that the same trajectory is obtained from the solution in Section 4.1 for the same parameters, with floating final time and $\alpha = 0.044685$. The cost for the motion calculated by the explicit solution is 23.2154, DIDO's cost is 22.8532. The cost difference here is a bit larger, but can be attributed to numerical errors, and the fact that DIDO's solution contains only 30 nodes.

The fourth case for the marginal cases and last to be presented is again for a fixed time, but with a higher bound on the velocity, so the bound is not reached. The bound on the velocity here is chosen to be high so the constraint will not become active, i.e. $V = 20[\mathrm{m/s}]$, and all other parameters are the same as in the previous simulation, i.e. $U = 10[\mathrm{m/s^2}], k = 0.05, x_0 = [0,0]^{\mathrm{T}}, x_f = [20,0]^{\mathrm{T}}, t_f = 5[\mathrm{s}]$. The result is presented in Figure 7. A perfect match between the two algorithms can be observed for this case also. Like in the second case presented in Figure 2, the system accelerates to a maximum velocity and then immediately decelerates to the final condition. The maximum velocity obtained

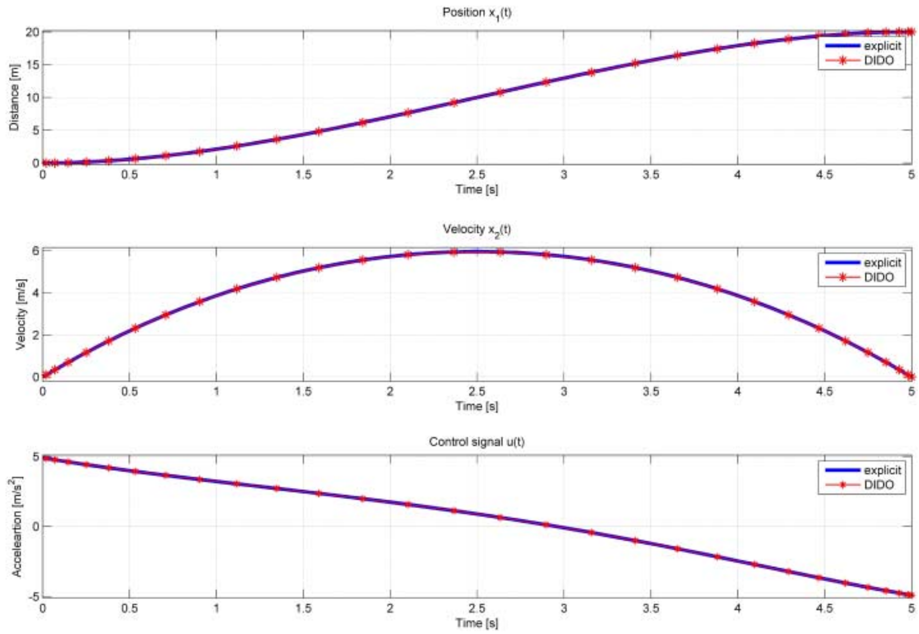

Figure 7. Marginal case with fixed final time, $t_f = 5$, minimum energy profile with inactive velocity bound constraint.

in this trajectory is $x_{2\_max} = 5.9552[\mathrm{m/s}]$ at $t_1 = t_2 = 2.5[\mathrm{s}]$. Again it is interesting to note that the same trajectory is obtained from the solution in Section 4.2 for the same parameters, with floating final time and $\alpha = 0.08326$. The cost for the motion calculated by the explicit solution is 21.0388, DIDO's cost is 20.0167. Again the difference in the cost is as in the previous simulation.

All simulation were done on the same platform, and the calculation times were measured. The explicit solution took approximately between 0.4–1.5 seconds, and DIDO's simulation took approximately between 45–120. The times vary due to the difference in complexity of the cases.

7. Conclusion

We have introduced the problem of combined optimal time energy control for a second-order system with quadratic drag, which can be used to describe many general systems for the purpose of trajectory planning. A solution was presented for the general case as well as two marginal cases, with supporting simulations comparing the solution to a widely used commercial solver. The method developed in this work aims to be incorporated as a module in a task planning solver which may need to call upon this module many times. Since this module will be called frequently, calculation times are critical. The solution presented here was faster on two times order, and more accurate than the commercial solver. This difference in calculation times can make this solution practically feasible for large task planning problems, where the commercial solver is too slow, even if the inaccuracies can be neglected for planning purposes.

Acknowledgements

We thank Prof. Jack Haddad for his assistance during the course of this research, and for comments that greatly improved the manuscript.

Disclosure statement

No potential conflict of interest was reported by the authors.

Funding

The first author was supported by the United States–Israel Binational Science Foundation (BSF) [grant number 2016007].

ORCID

Ayal Taitler http://orcid.org/0000-0003-3919-6883

References

[1] Coles AJ, Coles AI, Fox M, et al. Planning with continuous linear numeric change. J Artif Intel Res. 2012;44:1–96.
[2] Li HX, Williams BC. Generative planning for hybrid systems based on flow tubes. ICAPS; 2008. p. 206–213.
[3] Fernandez-Gonzalez E, Karpas E, Williams BC. Mixed discrete-continuous planning with convex optimization. Proceedings of the 31th Conference on Artificial Intelligence (AAAI'17); 2017. p. 4574–4580. Figure 1.
[4] Batchelor GK. An introduction to fluid dynamics. Cambridge: Cambridge University Press; 2000.
[5] Pontryagin LS. Mathematical theory of optimal processes. London: CRC Press; 1987.
[6] Hartl RF, Sethi SP, Vickson RG. A survey of the maximum principles for optimal control problems with state constraints. SIAM Rev. 1995;37(2):181–218.
[7] Ata AA. Optimal trajectory planning of manipulators: a review. J Eng Sci Technol. 2007;2(1):32–54.
[8] Berger A, Ioslovich I, Gutman PO. Time optimal trajectory planning with feedforward and friction compensation. American Control Conference (ACC), 2015; IEEE; 2015. p. 4143–4148.
[9] Ioslovich I, Gutman PO, Linker R, et al. Optimal rigid body precise displacement-minimization of electrical energy. IFAC-PapersOnLine. 2017;50(1):753–757.
[10] Wang Y, Ueda K, Bortoff SA. A Hamiltonian approach to compute an energy efficient trajectory for a servomotor system. Automatica. 2013;49(12):3550–3561.
[11] Ioslovich I, Gutman PO, Berger A, et al. On energy-optimal and time-optimal precise displacement of rigid body with friction. J Optim Theory Appl. 2017;172(2):466–480.
[12] Shiller Z. Time-energy optimal control of articulated systems with geometric path constraints. J Dyn Syst Meas Control. 1996;118(1):139–143.

[13] Verscheure D, Demeulenaere B, Swevers J, et al. Time-energy optimal path tracking for robots: a numerically efficient optimization approach. Advanced Motion Control, 2008. AMC'08. 10th IEEE International Workshop on; IEEE; 2008. p. 727–732.
[14] Ross IM. A primer on pontryagin's principle in optimal control. Oceanside: Collegiate Publishers; 2015.
[15] Ross IM, Karpenko M. A review of pseudospectral optimal control: from theory to flight. Annu Rev Control. 2012;36(2):182–197.
[16] Kirk DE. Optimal control theory: an introduction. New York: Courier Corporation; 2012.
[17] Arnold VI. Ordinary differential equations. Russia: Nauka; 1971.